

Contact boundary conditions and the Dyakonov–Shur instability in high electron mobility transistors


Frank J. Crowne

Citation: [Journal of Applied Physics](#) **82**, 1242 (1997); doi: 10.1063/1.365895

View online: <http://dx.doi.org/10.1063/1.365895>

View Table of Contents: <http://aip.scitation.org/toc/jap/82/3>

Published by the [American Institute of Physics](#)



Small Conferences. BIG Ideas.

Applied Physics
Reviews

SAVE THE DATE!
3D Bioprinting: Physical and Chemical Processes
May 2–3, 2017 • Winston Salem, NC, USA

Contact boundary conditions and the Dyakonov–Shur instability in high electron mobility transistors

Frank J. Crowne^{a)}

Department of Electrical Engineering, University of Maryland, College Park, Maryland 20742

(Received 21 January 1997; accepted for publication 29 April 1997)

Dyakonov and Shur have proposed a novel device structure based on dc biasing an ordinary high electron mobility transistor (HEMT) while subjecting it to unusual ac boundary conditions at its source and drain [M. Dyakonov and M. Shur, *Phys. Rev. Lett.* **71**, 2465 (1993)]. Under these conditions, the drifting two-dimensional electron gas within the HEMT channel acts as a trapped one-component plasma which exhibits damped normal-mode oscillations similar to those of an organ pipe under zero dc bias, and an unexpected instability and gain at large dc biases. In this article, the work of Dyakonov and Shur is generalized by allowing the plasma more hydrodynamic degrees of freedom. In particular, it is found that the description used by Dyakonov and Shur must be generalized to incorporate a more complicated picture of the plasma modes. © 1997 American Institute of Physics. [S0021-8979(97)02915-0]

A novel device structure has been proposed by Dyakonov and Shur¹ based on dc biasing an ordinary high electron mobility transistor (HEMT) while subjecting it to unusual ac boundary conditions at its source and drain. Under these conditions, the drifting two-dimensional electron gas (2DEG) acts as a trapped one-component plasma, whose dynamic behavior is strikingly similar to that of a tank of shallow water. In addition to exhibiting damped normal-mode oscillations similar to those of an organ pipe under zero dc bias, the trapped plasma has an unexpected instability and gain at large dc biases. The work of Dyakonov and Shur presupposes rather strong constraints on the 2DEG gas behavior in order to enforce the shallow-water analogy. In this article, the consequences of relaxing these constraints by allowing the plasma more hydrodynamic degrees of freedom are discussed. In particular, it is found that the “shallow-water” description used by Dyakonov and Shur must be generalized to incorporate a more complicated picture of the plasma modes.

I. THE DYAKONOV–SHUR MODEL

Following Dyakonov and Shur, let us start with the basic device geometry shown in Fig. 1 that is typical of HEMTs. The 2DEG is assumed to be infinitely thin compared to the other device dimensions, and an electrostatic potential exists everywhere inside the device (which we assume is an ordinary GaAs/AlGaAs heterostructure).

In their model, Dyakonov and Shur treat the 2DEG as a fluid that obeys the linearized microscopic equations of hydrodynamics.² They first assume that the 2DEG lies in the plane $z=h$, is infinitely extended parallel to the y axis in both directions, and has an unperturbed two-dimensional carrier density (carriers per unit area) n_0 and drift velocity v_0 arising from a dc source-to-drain bias. There is also an electrostatic potential $\varphi_0(y,z)$ defined everywhere within the structure, whereas the density and velocity are confined to the plane $z=h$ and are functions only of y . If the perturbed

(linearized) hydrodynamic variables are denoted by $n_1(y)$ (density), $v_1(y)$ (velocity), and $\varphi_1(y,z)$ (electrostatic potential), two hydrodynamic equations that can be written to describe their dynamic behavior are the continuity equation

$$-i\omega n_1 + v_0 \partial_y n_1 + n_0 \partial_y v_1 = 0,$$

and the equation of momentum conservation (the Euler equation)

$$-i\omega v_1 + v_0 \partial_y v_1 + \frac{c_p^2}{n_0} \partial_y n_1 = -\frac{e}{m} \partial_y \varphi_1(y,z) \Big|_{z=h},$$

where e is the electron charge and c_p is the “sound velocity.” This latter quantity, which enters in through the “pressure” term in the Euler equation, arises from the finite compressibility of the 2DEG. The force term on the right is derived by evaluating the y component of the electric field in the plane $z=h$. In their model, Dyakonov and Shur neglect the pressure term. They also avoid having to deal with the electrostatic potential by assuming that the density $n_1(y)$ is related to the potential by a “gate-to-channel” capacitance per unit area C , which is easily shown to equal ϵ/eh ; it is this step that allows them to invoke the shallow-water analogy. Then

$$n_1(y) = \frac{\epsilon}{eh} \varphi_1(y,h).$$

Let us assume that the y dependence of all quantities is that of a traveling wave, i.e., $e^{i(Ky - \omega t)}$, so that $n_1(y) = n_{1K} e^{i(Ky - \omega t)}$, $v_1(y) = v_{1K} e^{i(Ky - \omega t)}$. Then the assumptions of Dyakonov and Shur lead to the following two equations:

$$-i\omega n_{1K} + iKu_0 n_{1K} + iKn_0 u_{1K} = 0,$$

$$-i\omega v_{1K} + iKv_0 v_{1K} = -i \frac{e^2}{m\epsilon} n_{1K} hK.$$

Setting the determinant of these equations to zero yields the dispersion relation

$$(\omega - v_0 K)^2 = \frac{n_0 e^2 h}{m\epsilon} K^2$$

^{a)}Electronic mail: fcrowne@msc.arl.mil

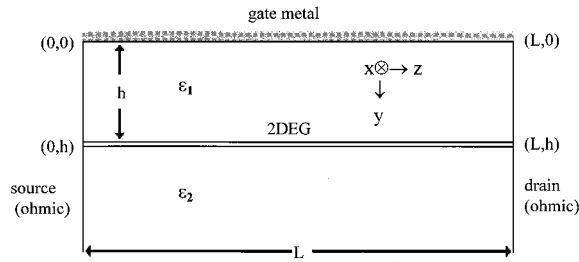


FIG. 1. HEMT device geometry.

or

$$\omega - v_0 K = \pm s K.$$

For $v_0 = 0$ this is clearly the equation of an “acoustic” wave with velocity $s = \sqrt{n_0 e^2 h / m \epsilon}$; nonzero values of v_0 Doppler shift this acoustic wave up or down in frequency. This says that the 2DEG acts like a moving acoustic medium, e.g., a compressible fluid or gas in motion. However, since $n = (\epsilon / e h) \phi$, we also have $n_0 = (\epsilon / e h) \phi_0$, which gives $s = \sqrt{e \phi_0 / m}$. This says that the velocity of these acoustic waves is tunable with gate voltage. For a gate voltage of 0.5 V, the value of s is around 10^8 cm/s, i.e., substantially higher than the saturation velocity of an electron in the 2DEG channel. This is one of the properties that makes the device interesting for high-frequency applications.

Such wavelike excitations of a 2DEG were well known to theorists³⁻⁶ in the 1970s, and were even observed experimentally by Tsui *et al.*⁷ at that time. The novel feature of Dyakonov and Shur’s work is their treatment of the finite geometry of the HEMT as a resonant cavity for these waves. To do so, they applied boundary conditions to the perturbed hydrodynamic variables at the ends of the 2DEG. The conditions they chose, which reflect the “external” electrical constraints imposed by the HEMT device environment,⁸ were either an ac electrical short [$\phi(y, h) = 0$] or an ac open [$j_1(y) = n_1(y) v_0 + n_0 v_1(y) = 0$]. Each of these conditions corresponds to a well-known acoustic boundary condition: the first to a closed pipe orifice or clamped string; the second to an open orifice or unclamped string. The choice made by Dyakonov and Shur was the somewhat unusual combination of an ac short at one end and an ac open at the other.

To solve the problem as they did, let us assume that

$$n_1(y) = A_+ e^{iK_+ y} + A_- e^{iK_- y},$$

i.e., a linear combination of forward and backward waves, where A_{\pm} are undetermined constants and

$$K_{\pm}(\omega) = \frac{\omega}{v_0 \pm s}.$$

Then in order to satisfy the continuity equation we must have

$$j_1(y) = \frac{\omega}{K_+} A_+ e^{iK_+ y} + \frac{\omega}{K_-} A_- e^{iK_- y}.$$

If the ac short occurs at the source end, then $n_1(y=0) = 0$, and so

$$A_+ + A_- = 0.$$

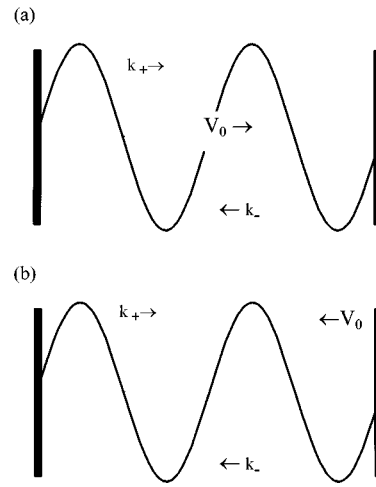


FIG. 2. Galilean transformation for the Doppler effect.

At the drain end the ac-open condition gives

$$\frac{\omega}{K_+} A_+ e^{iK_+ L} + \frac{\omega}{K_-} A_- e^{iK_- L} = 0.$$

These conditions together define an eigenvalue equation for the cavity frequency ω :

$$\frac{K_+(\omega)}{K_-(\omega)} = e^{i[K_+(\omega) - K_-(\omega)]L},$$

which can be reduced to the form

$$\exp\left(2i \frac{\omega L s}{s^2 - v_0^2}\right) = \frac{v_0 - s}{v_0 + s}.$$

When $v_0 = 0$, this reduces to $\exp[2i(\omega L/s)] + 1 = 0$, so that $\omega = (n + \frac{1}{2})\pi s/L$ is a real frequency, in fact the frequency of an open-topped organ pipe. For nonzero v_0 the right side is in fact the reflection coefficient at the drain boundary due to the ac-short condition, and is responsible for much of the unusual physics of the device. For $0 < v_0 < s$, this coefficient is negative and < 1 in absolute value, while the modulus of the left side is 1 for all real frequencies. Then the equation can only be satisfied if $\text{Im } \omega > 0$, which implies that the cavity oscillations grow with time. This means that the cavity mode is unstable, i.e., has gain.

Now, suppose that $v_0 > s$. Then we rewrite the equation

$$\exp\left(2i \frac{\omega L s}{v_0^2 - s^2}\right) = \frac{v_0 + s}{v_0 - s}.$$

In this case, the right side is > 1 , so that in order to satisfy the equation we must have $\text{Im } \omega < 0$, i.e., oscillations that decay with time.

To visualize the physics of this instability, it is convenient to transform to a frame of reference moving with the 2DEG, i.e., make a Galilean transformation from the lab (stationary frame) to a frame “at rest” with respect to the electrons of the 2DEG (see Fig. 2). In the new frame, we note that waves excited in the forward direction strike a boundary

that is moving backwards, i.e., towards them, while waves in the reverse direction must “catch up” with a boundary receding from them.

To understand the implications of this, consider the effect of the right-hand boundary alone on a forward wave for $0 < v_0 < s$. If we assume now that the “lab frame” moves with the 2DEG, the problem is solved by transforming to a frame where the boundary is stationary, and then essentially repeating the calculations of Dyakonov and Shur. After reversing this transformation to return to the lab frame, the solution that results is

$$f = A_0(e^{iK_+(x-ct)} + R e^{iK_-(x+ct)}),$$

where R depends on the detailed condition at the boundary. The point to notice here is that for this unbounded geometry there are *two* frequencies in the problem, not one. Therefore an attempt to find single-frequency modes of a bounded geometry will fail; the symptom of this failure is a complex value for the postulated frequency ω of the mode. The fact that the reflection coefficient R has a modulus greater than 1 causes growth of the signal due to multiple reflections.

If we now consider the case $v_0 > s$, the first thing we notice is that in the moving frame a wave reflected from the right-hand boundary *cannot* catch up with the left-hand boundary, which is moving at “supersonic” speed. This suggests that the origin of the attenuation in this case is simply the fact that only *one* reflection is possible. Note that no dissipation was included in the dynamic equations, so that the physics of the effect is obscure: it seems to resemble phase mixing, à la Landau damping, in that the energy of the cavity mode is returned to the dc flow. Note also that in the lab frame both reflected and incident waves are *forward* waves, i.e., no energy propagates back towards the drain.

II. ADDITIONAL DEGREES OF FREEDOM: INCLUSION OF VISCOSITY

Dyakonov and Shur have pointed out that an important factor in the dynamics of a 2DEG in a real HEMT is viscosity. Now we will show that viscosity changes the resonator problem in a profound way. When it is present, the hydrodynamic equations become

$$\begin{aligned} -i\omega n_1 + v_0 \partial_y n_1 + n_0 \partial_y v_1 &= 0, \\ -i\omega v_1 + v_0 \partial_y v_1 + \frac{c_p^2}{n_0} \partial_y n_1 &= -\frac{e}{m} \partial_y \varphi_1(y, z) \Big|_{z=h} + \nu \partial_y^2 v_1, \end{aligned}$$

where ν is the kinematic viscosity.² The same kind of manipulations as above lead to the infinite-gas dispersion relation

$$(\omega - v_0 K)(\omega - v_0 K + i\nu K^2) = (s^2 + c_p^2) K^2.$$

This equation is now cubic in K , i.e., there are three frequency-dependent complex propagation constants.

With three values of K , we now must write the density as follows:

$$n_1(y) = A_+ e^{iK_+ y} + A_- e^{iK_- y} + A_\nu e^{iK_\nu y},$$

so that there are now three arbitrary constants to be found. It appears that an extra boundary condition is now needed.

Remarkably, the extra condition we need is at hand. In an ordinary HEMT, like most field-effect transistors, the source and drain contacts are designed to be ohmic. Near these contacts, the 2DEG can be shown to behave like an $n-n^+$ junction, for which the dc charge density near the contact point is determined by the high-density electron gas in the three-dimensional (3D) region. This suggests that the ac charge density should not vary at the ac frequency, i.e., that

$$n_1(0) = n_1(L) = 0.$$

At the source end, this condition is redundant, since $n_1(y) = (\epsilon/eh)\varphi_1(y, h)$. However, at the drain end the conditions $n_1(y=L)=0$ and $j_1(y=L)=0$ are entirely independent. This means that there are three boundary conditions, and we have (rather fortuitously) enough conditions to solve the problem.

The three conditions give the equations

$$A_+ + A_- + A_\nu = 0,$$

$$A_+ \zeta_+ + A_- \zeta_- + A_\nu \zeta_\nu = 0,$$

$$\frac{\omega}{K_+} A_+ \zeta_+ + \frac{\omega}{K_-} A_- \zeta_- + \frac{\omega}{K_\nu} A_\nu \zeta_\nu = 0,$$

where $\zeta_i = e^{iK_i z}$ and $i = +, -, \nu$. We solve the system by setting its determinant to zero:

$$\begin{vmatrix} 1 & 1 & 1 \\ \zeta_+ & \zeta_- & \zeta_\nu \\ \frac{\zeta_+}{K_+} & \frac{\zeta_-}{K_-} & \frac{\zeta_\nu}{K_\nu} \end{vmatrix} = 0,$$

which gives

$$\frac{\zeta_+}{K_+} (\zeta_\nu - \zeta_-) + \frac{\zeta_-}{K_-} (\zeta_+ - \zeta_\nu) + \frac{\zeta_\nu}{K_\nu} (\zeta_- - \zeta_+) = 0.$$

When used with the dispersion relation for the $K(\omega)$, this equation determines the resonator frequency ω . The presence of the extra K value indicates that the number of degrees of freedom has increased. Rather than attempt to find these frequencies here, let us instead go on to the more general case discussed in Sec. III, where this problem is compounded.

III. GENERALIZATION OF THE DYAKONOV-SHUR MODEL TO AN ARBITRARY DEVICE GEOMETRY

A. The 2DEG at an arbitrary distance from the gate

The assumption that the density $n_1(y)$ is linearly related to the electrostatic potential by a “gate-to-channel” capacitance per unit area can be relaxed by introducing the Poisson equation for the potential in the device volume:

$$(\partial_y^2 + \partial_z^2) \varphi_1(y, z) = -\frac{e}{\epsilon} n_1(y) \delta(z-h).$$

Now the potential is no longer proportional to the local density, but is a degree of freedom in its own right. The addition of a degree of freedom should affect the resonator problem in the same way that addition of viscosity did.

Because of the δ function, the potential $\varphi_1(y,z)$ will have a discontinuity in its z derivative across the 2DEG. The boundary condition on $\varphi_1(y,z)$ at the gate $z=0$ is $\varphi_1(y,0)=0$, i.e., the gate is an equipotential. Then a wavelike solution to the Poisson equation that satisfies this boundary condition along with the condition $\lim_{z \rightarrow \infty} \varphi_1(y,z)=0$ is

$$\varphi_1(y,z) = \tilde{\varphi}_1(K,z) e^{iKy},$$

where

$$\tilde{\varphi}_1(K,z) = \frac{e}{2\epsilon K} n_1(y) e^{-Kh} \sinh Kz, \quad z \in (0,h),$$

and

$$= \frac{e}{2\epsilon K} n_1(y) e^{-Kz} \sinh Kh, \quad z \in (h,\infty);$$

here $n_1(y) = n_{1K} e^{iKy}$. This form of the potential implies that

$$\partial_y \varphi_1(y,z)|_{z=h} = iK \tilde{\varphi}_1(K,h) e^{iKy}.$$

Since

$$\tilde{\varphi}_1(K,h) = \frac{e}{2\epsilon K} n_1(y) (1 - e^{-2Kh}),$$

the hydrodynamic equations become

$$(\omega - v_0 K) n_1 = n_0 K v_1,$$

$$(\omega - v_0 K) v_1 = \frac{e^2}{2m\epsilon} (1 - e^{-2Kh}) n_1,$$

which leads to the dispersion relation

$$(\omega - v_0 K)^2 = \frac{n_0 e^2}{2m\epsilon} K (1 - e^{-2Kh}).$$

This reduces to the expression given in Ref. 7 for the case $v_0=0$. At long wavelengths ($Kh \ll 1$) we can write

$$1 - e^{-2Kh} \approx 2Kh,$$

which gives

$$(\omega - v_0 K)^2 = \frac{n_0 e^2 h}{m\epsilon} K^2,$$

i.e., the original dispersion relation of Dyakonov and Shur.

In general we must now solve a transcendental equation to find the function $K(\omega)$ for the unbounded case. Our results for the viscous 2DEG indicate that, before we set up the resonator problem, we must ask how many roots the unbounded dispersion relation has. In the analysis of Dyakonov and Shur, there were only two roots, corresponding to a forward and a backward wave, and therefore only two boundary conditions were required for the resonator, which could be chosen in a natural way. What happens in the more general case under discussion here?

A simple graphical construction shows that the number of roots of the dispersion relation has doubled, and that this situation persists even when $Kh \ll 1$, i.e., the Dyakonov–Shur limit. Consider the two functions

$$f_1(K) = \frac{n_0 e^2}{2m\epsilon} K (1 - e^{-2Kh}),$$

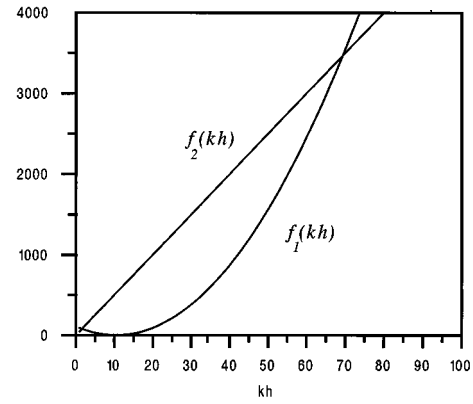


FIG. 3. Graphical solution to bulk dispersion relation for gated-HEMT plasmons.

and

$$f_2(K) = (\omega - v_0 K)^2.$$

The dispersion relation is satisfied for those values of K where these two functions intersect. Figure 3 shows a plot of these two functions for values of the other parameters that are typical of the Dyakonov–Shur limit. Note that there are two solutions for $K(\omega)$, one with Kh small and one with Kh large. It will be shown below that the former root corresponds to both Dyakonov–Shur roots, while the latter, which goes to infinity as $h \rightarrow \infty$, adds two more roots.

B. The isolated drifting 2DEG

The complexity of the general transcendental equation is a major hindrance to analysis of the resonator problem. Fortunately, in addition to the limit $Kh \ll 1$ there is another limit, that Dyakonov and Shur refer to as the “deep-water limit,” for which the 2DEG dispersion relation can be solved exactly: the limit $Kh \gg 1$. Here the exponential term drops out and the dispersion equation becomes

$$(\omega - v_0 K)^2 = \frac{n_0 e^2}{2m\epsilon} K \equiv \Lambda K,$$

where $\Lambda = n_0 e^2 / 2m\epsilon$. For $v_0=0$ this dispersion relation becomes $\omega^2 = \Lambda K$, an expression first derived by Ferrel⁹ and later discussed in much detail by Fetter¹⁰ in 1973, who described it as a “two-dimensional (2D) plasmon.” Its peculiar dispersion characteristics have often been noted, in particular its (physically unreasonable) infinite group velocity $d\omega/dK$ as $K \rightarrow 0$.

At this point some caution is warranted regarding the meaning of some terms in this problem, particularly the labels “forward” and “backward” wave. In a fully 2D problem we would treat the Doppler shift by allowing the direction of propagation of the wave \mathbf{K} to make an arbitrary angle θ with the flow, as shown in Fig. 4. Under these conditions, it is the magnitude of the vector $|\mathbf{K}|$ that enters into the problem:

$$\omega = (v_0 \cos \theta + s) |\mathbf{K}|.$$

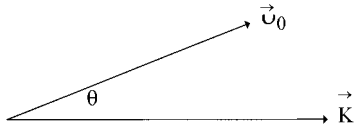


FIG. 4. Full 2D geometry for Doppler-shifted plasmons.

For $\theta=0$ \mathbf{K} specifies a “forward wave,” for $\theta=\pi$ the wave is “backward.” However, there is only *one* value of $|\mathbf{K}|$ for each ω and θ .

Things are otherwise when we turn to the 2D plasmon dispersion relation, which we should write in the form

$$(\omega - |\mathbf{K}|v_0 \cos \theta)^2 = \Lambda |\mathbf{K}|.$$

Solving for $|\mathbf{K}|$, we find that

$$|\mathbf{K}| = \frac{\omega + \frac{\Lambda}{2v_0 \cos \theta} \pm \sqrt{\left(\omega + \frac{\Lambda}{2v_0 \cos \theta}\right)^2 - \omega^2}}{v_0 \cos \theta},$$

i.e., there are now *two* values of $|\mathbf{K}|$ for each ω and θ . This means that for $\theta=0$ there are two “forward” waves, and two “backward” waves for $\theta=\pi$.

Some reflection reveals that things are actually even more complicated than this: since we are allowing complex values of $|\mathbf{K}|$, we have no guarantee that $\text{Re}|\mathbf{K}| > 0$, which we require in order that our Poisson-equation solution be bounded in the z direction. This suggests that $|\mathbf{K}|$ may not be the best variable to use in describing the propagation of these waves.

A better way to address this problem is to rewrite our three basic hydrodynamic equations in rectangular coordinates:

$$-i\omega n_1 + (\mathbf{v}_0 \cdot \nabla_\perp) n_1 + n_0 (\nabla_\perp \cdot \mathbf{v}_1) = 0,$$

$$-i\omega \mathbf{v}_1 + (\mathbf{v}_0 \cdot \nabla_\perp) \mathbf{v}_1 = \frac{e}{m} \nabla_\perp \varphi_1,$$

$$(\nabla_\perp^2 + \partial_z^2) \varphi_1(x, y, z) = -\frac{e}{\epsilon} n_1(x, y) \delta(z-h),$$

where ∇_\perp denotes the gradient in the plane of the layer, i.e., the vector (∂_x, ∂_y) . The mode hydrodynamic velocities are now vectors in the 2DEG plane: $\mathbf{v}_0 = (0, v_0)$, $\mathbf{v}_1 = (v_x, v_y)$, choosing the y axis for the dc flow as before. We will assume that the modes are now nontrivial functions of both x and y , characterized by ordinary propagation in the x direction, i.e., an x dependence of the form $e^{iK_x x}$ with K_x real, plus a y dependence of the form $e^{iK_y y}$ where K_y can have an arbitrary (complex) value. We can still identify a wave with $\text{Re } K_y > 0$ as a forward wave, and one with $\text{Re } K_y < 0$ as a backward wave. Then the equations given above become

$$(\omega - K_y v_0) n_1 = n_0 (K_x v_x + K_y v_y),$$

$$(\omega - K_y v_0) v_x = -\frac{e}{m} K_x \varphi_1(z=h),$$

$$(\omega - K_y v_0) v_y = -\frac{e}{m} K_y \varphi_1(z=h),$$

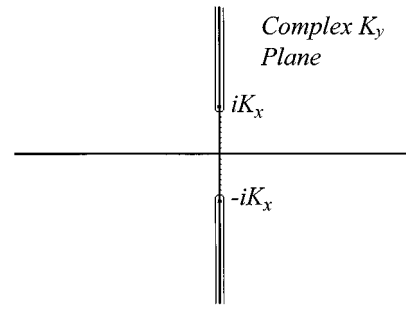


FIG. 5. Complex-plane definition of the function $\sqrt{K_y^2 + K_x^2}$.

$$(\partial_z^2 - K_x^2 - K_y^2) \varphi_1(z) = -\frac{e}{\epsilon} n_1 \delta(z-h).$$

Substituting the velocity expressions into the density equation gives

$$(\omega - K_y v_0)^2 n_1 = -\frac{n_0 e}{m} (K_x^2 + K_y^2) \varphi_1(z=h),$$

while solving the Poisson equation gives

$$\varphi_1(z) = -\frac{e n_1}{2\epsilon \sqrt{K_x^2 + K_y^2}} \exp[-|z-h| \sqrt{K_x^2 + K_y^2}],$$

and hence

$$\varphi_1(z=h) = -\frac{e n_1}{2\epsilon \sqrt{K_x^2 + K_y^2}}.$$

This gives the dispersion relation in its final form:

$$(\omega - K_y v_0)^2 = \frac{n_0 e^2}{2\epsilon m} \sqrt{K_x^2 + K_y^2}.$$

The reason for doing all this is that the function $\tilde{K}(K_y) = \sqrt{K_x^2 + K_y^2}$, which determines whether the exponential in our Poisson solution is indeed bounded in z , has the extremely useful property $\text{Re } \tilde{K}(K_y) > 0$ for all complex values of K_y if it is defined in the K_y plane as shown in Fig. 5. Here the choice of branch cuts, which is made so that $\arg(K_y + iK_x) \in (-3\pi/2, \pi/2)$ and $\arg(K_y - iK_x) \in (-\pi/2, 3\pi/2)$, is critical to defining the analytic function $\tilde{K}(K_y)$ so that its real part is positive.

Once all this is done, we can solve the dispersion relation for K_y without compromising our solution to the Poisson equation. To do so, we square the dispersion relation to obtain

$$(K_y - k_0)^4 = 2\xi(K_x^2 + K_y^2),$$

where $\xi = \Lambda/2v_0^2$ and $k_0 = \omega/v_0$. The quantity ξ^{-1} defines an intrinsic length scale for the plasma waves. It will be shown below that the ratio of this length to the gate length controls the gain and dispersion of these waves. Introducing the notation $u = K_y - k_0$ leads to the following quartic equation:

$$u^4 = 4\xi^2([u + k_0]^2 + K_x^2).$$

The four roots of this equation (in general complex) must be tested to ensure that they actually satisfy the unsquared dispersion relation, which in this notation becomes

$$u^2 = 2\xi\sqrt{(u+k_0)^2 + K_x^2}.$$

Setting $K_x = 0$ now gives

$$u^2 = 2\xi|u + k_0|,$$

where any ambiguity in the meaning of the absolute value can be resolved by returning to the $K_x \neq 0$ case. Solving this equation leads to the following four roots:

$$K_x^{(1)} = k_0 + \xi + \sqrt{\xi(\xi + 2k_0)},$$

$$K_x^{(2)} = k_0 + \xi - \sqrt{\xi(\xi + 2k_0)},$$

$$K_x^{(3)} = k_0 - \xi + \sqrt{\xi(\xi - 2k_0)},$$

$$K_x^{(4)} = k_0 - \xi - \sqrt{\xi(\xi - 2k_0)}.$$

In the limit $v_0 \rightarrow 0$ it is easy to show that

$$K_x^{(1)} \approx 2\xi \rightarrow \infty,$$

$$K_x^{(2)} \approx \frac{\omega^2}{\Lambda},$$

$$K_x^{(3)} \approx -\frac{\omega^2}{\Lambda},$$

$$K_x^{(4)} \approx -2\xi \rightarrow -\infty,$$

i.e., the $K_x^{(1,2)}$ correspond to forward waves, the $K_x^{(3,4)}$ to backward waves. The roots $K_x^{(2,3)}$ clearly reduce to the “standard” expression given by Ferrel for a stationary 2DEG, the other two roots $K_x^{(1,4)}$ oscillate infinitely rapidly in this limit, and are presumably damped out by viscosity.

As v_0 increases, ξ decreases more rapidly than k_0 , so that eventually we reach a point where $k_0 > \xi/2$. At this point, the waves $K_x^{(3,4)}$ develop imaginary parts with opposite signs, indicating that the flow has become convectively unstable. The exponentially damped fields around the 2DEG begin to oscillate in the z direction, and extend further and further out into the surrounding space. Further increases in v_0 eventually give $k_0 > \xi$. At this point, the fields around the 2DEG are no longer bound, indicating that the system is absolutely unstable since no propagation transverse to the 2DEG is possible within an electrostatic problem.

Let us suppose now that we fix v_0 and vary the frequency. The $\omega \rightarrow 0$ limit is the same as the $v_0 \rightarrow 0$ limit, so that the limiting expressions given above hold. In particular, the dc limit shows evidence of a “charge density wave,” i.e., an inhomogeneous state of the *static* 2DEG with wave number 2ξ , which is now a finite quantity. This dc “wave,” which will not be discussed here, appears to arise from an interaction between the dispersive Ferrel-type plasmon and the isentropic “streaming” characteristic mentioned by Landau and Lifshits,² which carries time-dependent perturbations convectively away from their source, thereby generating “waves” that move with the flow velocity. The conditions $k_0 > \xi/2$, $k_0 > \xi$ are now frequency conditions, which will play an important role in the resonator problem.

IV. THE RESONATOR PROBLEM

Let us revisit the Dyakonov–Shur resonator. We write the two forward roots of the dispersion relation as $K_{f\pm}$ and the two backward roots as $K_{b\pm}$, i.e.,

$$K_{f+} = K_x^{(1)} = k_0 + \xi + \sqrt{\xi(\xi + 2k_0)},$$

$$K_{f-} = K_x^{(2)} = k_0 + \xi - \sqrt{\xi(\xi + 2k_0)},$$

$$K_{b+} = -K_x^{(3)} = -k_0 + \xi - \sqrt{\xi(\xi - 2k_0)},$$

$$K_{b-} = -K_x^{(4)} = -k_0 + \xi + \sqrt{\xi(\xi - 2k_0)},$$

and the plasma density as

$$n_1(y) = N_{f+} e^{iK_{f+}y} + N_{f-} e^{iK_{f-}y} + N_{b+} e^{-iK_{b+}y} + N_{b-} e^{-iK_{b-}y}.$$

This choice of signs for the K_i emphasizes the forward and backward nature of the waves that make up the disturbance. We now have *four* unknown coefficients to find. The corresponding electrostatic potential is

$$\varphi_1(y) = \frac{e}{2\epsilon} \left(\frac{1}{K_{f+}} N_{f+} e^{iK_{f+}y} + \frac{1}{K_{f-}} N_{f-} e^{iK_{f-}y} + \frac{1}{K_{b+}} N_{b+} e^{-iK_{b+}y} + \frac{1}{K_{b-}} N_{b-} e^{-iK_{b-}y} \right),$$

the electric field is

$$\partial_y \varphi_1(y) = \frac{e}{2\epsilon} (N_{f+} e^{iK_{f+}y} + N_{f-} e^{iK_{f-}y} - N_{b+} e^{-iK_{b+}y} - N_{b-} e^{-iK_{b-}y}),$$

and the current is

$$j_1(y) = -e \left(\frac{\omega}{K_{f+}} N_{f+} e^{iK_{f+}y} + \frac{\omega}{K_{f-}} N_{f-} e^{iK_{f-}y} - \frac{\omega}{K_{b+}} N_{b+} e^{-iK_{b+}y} - \frac{\omega}{K_{b-}} N_{b-} e^{-iK_{b-}y} \right).$$

Note that the potential is no longer simply related to the density. Then we need to impose four boundary conditions. Two are as before.

I. Voltage clamping at $y=0$: $\varphi_1(y=0)=0$, so

$$\frac{1}{K_{f+}} N_{f+} + \frac{1}{K_{f-}} N_{f-} + \frac{1}{K_{b+}} N_{b+} + \frac{1}{K_{b-}} N_{b-} = 0.$$

II. Vanishing of the current at $y=L$: $j_1(y=L)=0$, so (dropping a factor of $-e\omega$)

$$\frac{1}{K_{f+}} N_{f+} e^{iK_{f+}L} + \frac{1}{K_{f-}} N_{f-} e^{iK_{f-}L} - \frac{1}{K_{b+}} N_{b+} e^{-iK_{b+}L} - \frac{1}{K_{b-}} N_{b-} e^{-iK_{b-}L} = 0.$$

But what do we use for the other two conditions? The literature on ohmic contacts^{10–14} suggests several possible choices based on the microscopic conditions near each contact. As discussed above for the case of a viscous 2DEG, one way to introduce ohmic behavior is to set the ac charge den-

sity equal to zero. Another simpler choice is to assume that a “perfect” ohmic contact cannot support an electric field across it. This leads to a plausible second set of boundary conditions, namely, that the electric field should vanish at the source and drain ends of the 2DEG. The argument here is that within the contact regions no electric fields can exist, so that continuity of the field would imply zero field immediately *inside* the 2DEG as well. This is also similar to the zero-pressure gradient condition at the mouth of an open pipe; because it can flow freely in and out, the fluid cannot support any force across the opening. Note that the vanishing-potential and vanishing-electric field conditions are emphatically *not* equivalent within the Dyakonov–Shur model, so we should not expect to recover their results.

In this article we will choose the vanishing-electric field conditions.

III. Ohmic behavior at $y=0$: $\partial_y \varphi_1(y=0)=0$, which implies

$$N_{f+} + N_{f-} - N_{b+} - N_{b-} = 0.$$

IV. Ohmic behavior at $y=L$: $\partial_y \varphi_1(y=L)=0$, so

$$N_{f+} e^{iK_{f+}L} + N_{f-} e^{iK_{f-}L} - N_{b+} e^{-iK_{b+}L} - N_{b-} e^{-iK_{b-}L} = 0.$$

We now set the determinant of this system of equations to zero:

$$\begin{vmatrix} K_{f-} & K_{f+} & K_{b-} & K_{b+} \\ 1 & 1 & -1 & -1 \\ \zeta_{f+} & \zeta_{f-} & -\zeta_{b+}^* & -\zeta_{b-}^* \\ K_{f-}\zeta_{f+} & K_{f+}\zeta_{f-} & -K_{b-}\zeta_{b+}^* & -K_{b+}\zeta_{b-}^* \end{vmatrix} = 0,$$

where $\zeta_i = e^{iK_i z}$; the fact that $K_{f+}K_{f-} = K_{b+}K_{b-} = \omega^2/v_0^2$ was used to simplify the determinant somewhat.

The detailed evaluation of this determinant is relegated to the Appendix. Introducing the notation

$$\Delta = \xi L = \frac{\Lambda L}{2v_0^2}, \quad z = \frac{k_0}{\xi} = \frac{2\omega v_0}{\Lambda},$$

we can write the dispersion relation in its final form:

$$(1+z) \left(\frac{\sin \Delta \sqrt{1+2z}}{\sqrt{1+2z}} \cos \Delta \sqrt{1-2z} \right) + (1-z) \times \left(\frac{\sin \Delta \sqrt{1-2z}}{\sqrt{1-2z}} \cos \Delta \sqrt{1+2z} \right) + \sin 2\Delta = 0, \quad (1)$$

which defines a complex function $z(\Delta)$.

In the limit of small Δ it is possible to solve for $z(\Delta)$ by making the expansion

$$z = \frac{z_0}{\Delta} + z_1 + \mathcal{O}(\Delta).$$

Despite the singular behavior of $z(\Delta)$, the arguments of the trigonometric functions are small, which aids in the expansion procedure. The coefficients can be found in the usual way; it turns out that $z_1=0$, and the final result is

$$z = \frac{\pm i\sqrt{3}}{\Delta} + \mathcal{O}(\Delta).$$

If we go to dimensional units, this becomes

$$\tilde{\omega} = \pm i\sqrt{3} \frac{v_0}{L},$$

i.e., the frequency is pure imaginary. Since both signs of $\text{Im } \omega$ are allowed, the device exhibits gain at these frequencies. Note that the gain of the device is determined by the transit time across the gate.

For other values of Δ Eq. (1) requires a numerical solution, since complex values of ω must be considered. A 2D simplex routine was used to solve it, which minimizes the real-valued function $|f(z, \Delta)|^2$ of the two real variables $\text{Re } z$ and $\text{Im } z$; when this minimum is zero, we have a root. Note that the function is even in z , so that $-z$ is a root whenever z is.

The function $z(\Delta)$, whose real and imaginary parts are plotted in Figs. 6(a) and 6(b), has the following features.

- (1) For small Δ , $z(\Delta)$ diverges and is pure imaginary, as we proved above. Since this limit corresponds to large v_0 , we may conclude that the “deep-water” 2D plasma, unlike the “shallow-water” 2D plasma, is unstable at *high* drift velocities.
- (2) As Δ increases from zero, the roots first switch from pure imaginary to real, and then alternate in a bewildering way between real ($\text{Im } z=0$), imaginary ($\text{Re } z=0$), and complex values (both $\text{Re } z$ and $\text{Im } z$ nonzero). The existence of the first two classes of roots will be verified analytically in Sec. V. It is not hard to see that $z=0$ is a solution whenever Δ satisfies the equation

$$\sin 2\Delta = 0,$$

i.e., $\Delta = \Delta_m \pi/2$. The first time this happens is for $m=1$, at which $\Delta_1 = 1.57$. These solutions correspond to the zero-frequency charge density waves (i.e., “soft modes”) mentioned above.

The regions where $\text{Im } z$ is nonzero get smaller and smaller as Δ increases. This is a satisfying result since large Δ means small v_0 . It is interesting that there does not seem to be a “threshold” in v_0 below which there is no instability at all; nonzero values of Δ_m persist down to zero velocity, although the unstable regions around them shrink to zero. This is probably associated with the infinite group velocity of the Ferrel plasmons.

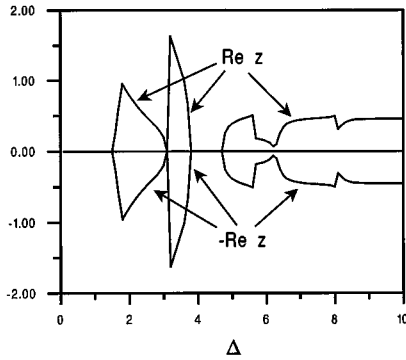
Figures 6(a) and 6(b) show the overall behavior of $\text{Re } z$ and $\text{Im } z$ for $0 < \Delta < 10$ and the following choice of 2DEG parameters:

$$n_0 = 10^{11} \text{ cm}^{-2}, \quad v_0 = 3 \times 10^6 \text{ cm/s}, \quad \epsilon = 13.1,$$

$$m^* = 0.067 m_0.$$

Note that this plot is equivalent to a plot of frequency versus gate length. In Figs. 6(a) and 6(b) $\text{Re } z$ and $-\text{Re } z$ are plotted together, along with $\text{Im } z$ and $-\text{Im } z$; superimposing these four quantities shows the way the branches match. The complexity of the spectrum is evident. Figure 7 is a detailed view of the neighborhood of the first transition point $\Delta_1 = \pi/2$. Note also the smooth transitions from one kind of root to another.

(a)



(b)

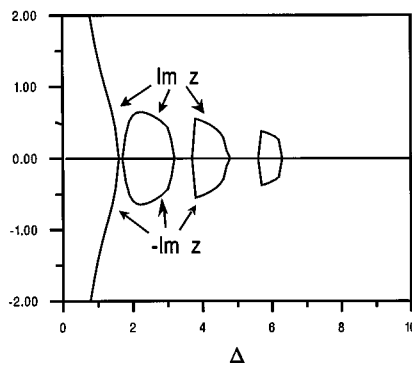


FIG. 6. Complex function $z(\Delta)$ plotted vs Δ . (a) Real part of z ; (b) imaginary part of z .

V. COMPARISON WITH THE DYAKONOV–SHUR MODEL

We expect the results presented here to differ strongly from those of Ref. 1 due to the different boundary conditions applied; unfortunately, they also differ trivially because the model of Dyakonov and Shur requires the proximity of a

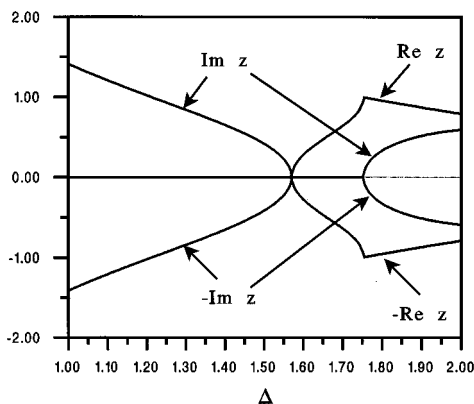


FIG. 7. Close up view of the function $z(\Delta)$ ($\pm \text{Re } z$ and $\pm \text{Im } z$) near $\Delta = \pi/2$.

Mode Modulus

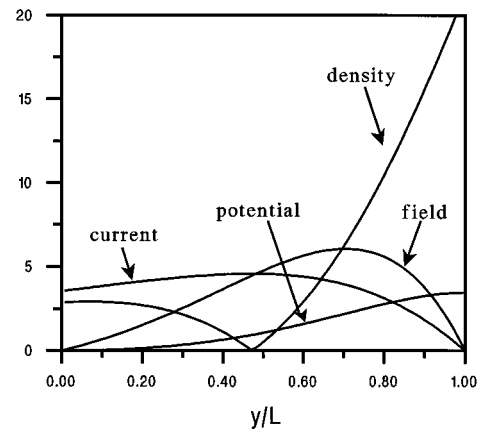


FIG. 8. Generalized plasma-mode hydrodynamic variables for $\Delta = 1$.

gate, whereas in the case discussed here the gate is absent. Nevertheless, it is worthwhile to at least compare the predicted mode shapes for the two models. Figures 8–16 show three sets of plots of the spatial variation of the hydrodynamic variables along the 2DEG for the (unnormalized) modes with values $\Delta = 1$, $\Delta = 1.57 \approx \pi/2$, and $\Delta = 2$. In each set the spatial variations for the “generalized” modes discussed in this article are plotted along with the two lowest-frequency modes from the Dyakonov–Shur model, assuming a gate-to-2DEG distance $h = 0.1L$, where L is the gate length (i.e., source-to-drain spacing) of the HEMT, i.e., a fixed “aspect ratio;” note that changing Δ changes L . There are several things to note about these plots.

- (1) The generalized modes exhibit a new overall structure in this range of Δ , one that is entirely absent from the Dyakonov–Shur modes.
- (2) A striking feature of the generalized modes at the special point $\Delta_1 = \pi/2$ is the apparent presence of current nodes at *both* ends of the device, even though the boundary condition only enforces this at the drain end. The Dyakonov–Shur modes exhibit no such behavior.

Mode Amplitude

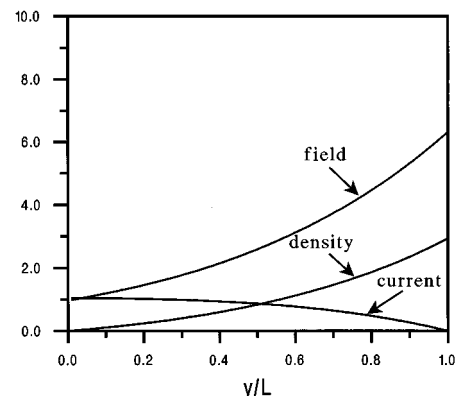


FIG. 9. Hydrodynamic variables for the $n=0$ Dyakonov–Shur mode, $\Delta = 1$.

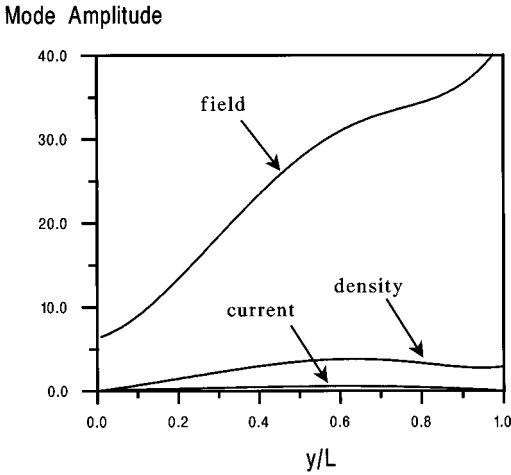


FIG. 10. Hydrodynamic variables for the $n=1$ Dyakonov-Shur mode, $\Delta=1$.

- (3) For the generalized modes, the density has a node near the device center for all three values of Δ , unlike either of the Dyakonov-Shur modes (although the $n=1$ modes show some oscillatory behavior). Note that the density is not proportional to the potential for the generalized modes, again in contrast to the Dyakonov-Shur modes.
- (4) For the generalized modes, peaks in the various quantities shift toward the source for $\Delta > \pi/2$, and toward the drain for $\Delta < \pi/2$.

VI. THE ROLE OF DISSIPATION

It is a nontrivial task to include dissipation in a drifting 2DEG, although Dyakonov and Shur attempt to address the problem in Ref. 1. The simplest type of dissipation to treat involves collisions with heavy impurities, which change the Euler equation to

$$-i\omega v_1 + \frac{1}{\tau} v_1 + v_0 \partial_y v_1 = -\frac{e}{m} \partial_y \varphi_1(y, z) \Big|_{z=h},$$

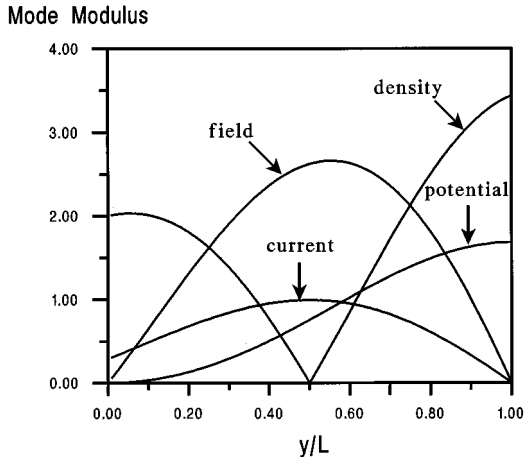


FIG. 11. Generalized plasma-mode hydrodynamic variables for $\Delta=\pi/2$.

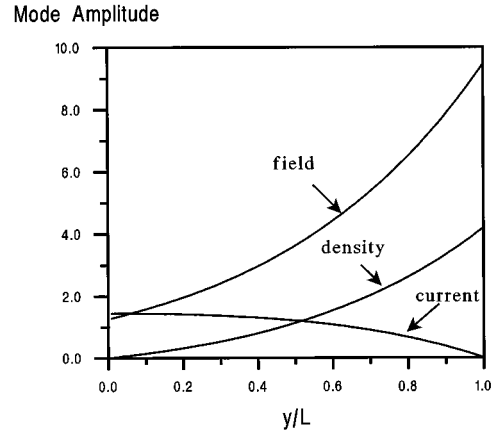


FIG. 12. Hydrodynamic variables for the $n=0$ Dyakonov-Shur mode, $\Delta=\pi/2$.

here τ is the collision time, which determines the momentum relaxation. The next order of complexity would be addition of viscosity, which is related to energy relaxation. However, the correct treatment of energy relaxation requires that we introduce viscosity simultaneously with thermal conduction, and the resulting physics is too rich to treat in anything less than a separate publication.

Here we will be content to treat the case of impurity scattering, which changes the deep-water dispersion relation to

$$(\omega - K_y v_0) \left(\omega + \frac{i}{\tau} - K_y v_0 \right) = \frac{n_0 e^2}{2 \epsilon m} \sqrt{K_x^2 + K_y^2}.$$

Using the same substitutions as in the undamped case, we reduce this to the following equation:

$$u(u + i\kappa) = 2\xi|u + k_0|,$$

where $\kappa = 1/\nu_0 \tau$ is the “drift length” of a carrier between scatterings. As before, when u is complex we interpret the function $|u|$ as $\sqrt{u^2}$ and take the branch with positive real part. This equation can once more be solved exactly, to give four roots:

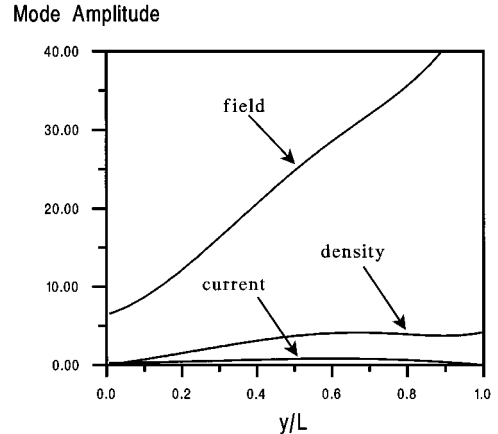


FIG. 13. Hydrodynamic variables for the $n=1$ Dyakonov-Shur mode, $\Delta=\pi/2$.

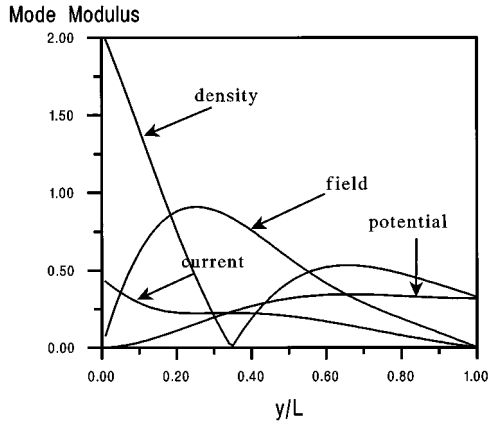


FIG. 14. Generalized plasma-mode hydrodynamic variables for $\Delta=2$.

$$K_{f+} = k_0 + \xi + \frac{1}{2} i\kappa + \sqrt{\left(\xi + \frac{1}{2} i\kappa\right)^2 + 2k_0\xi},$$

$$K_{f-} = k_0 + \xi + \frac{1}{2} i\kappa - \sqrt{\left(\xi + \frac{1}{2} i\kappa\right)^2 + 2k_0\xi},$$

$$K_{b+} = -k_0 + \xi - \frac{1}{2} i\kappa + \sqrt{\left(\xi - \frac{1}{2} i\kappa\right)^2 - 2k_0\xi},$$

$$K_{b-} = -k_0 + \xi - \frac{1}{2} i\kappa - \sqrt{\left(\xi - \frac{1}{2} i\kappa\right)^2 - 2k_0\xi}.$$

These roots are plotted in Figs. 17 and 18 over a wide frequency range for the same 2DEG parameters as in Fig. 6. In Fig. 17, the relaxation time was $\tau=10^{-7}$ s (corresponding to a collisionless 2DEG), and in Fig. 18, the relaxation time was $\tau=10^{-13}$ s (corresponding to a GaAs mobility of $2600 \text{ cm}^2/\text{V s}$). Note that for these device parameters the system exhibits some gain at all frequencies for at least one of the four waves whenever the velocity v_0 is nonzero. A similar prediction is well known for classical three-dimensional plasmas, where the gain effect is described as a “collision-induced” instability.¹⁵ Also worth noting is the fact that whereas at low frequencies three of the waves are forward

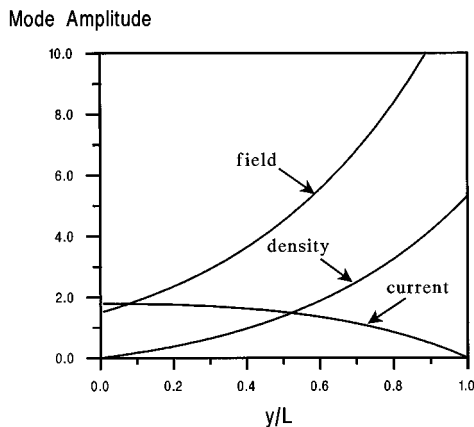


FIG. 15. Hydrodynamic variables for the $n=0$ Dyakonov–Shur mode, $\Delta=2$.

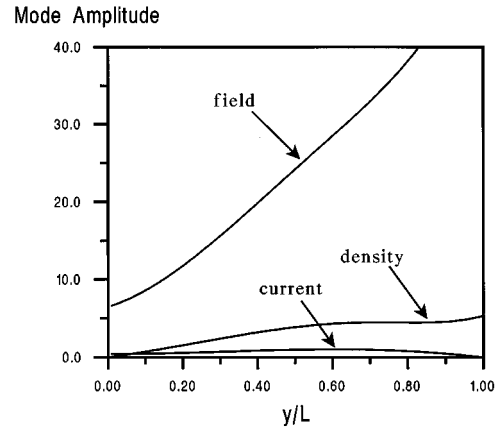
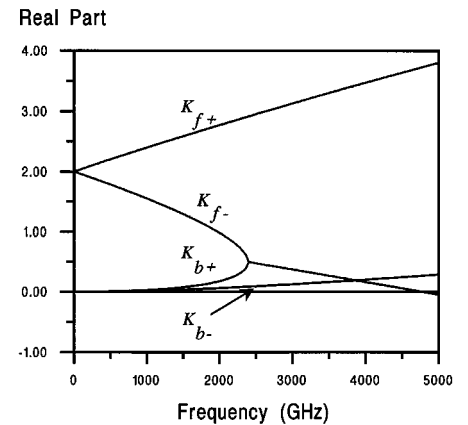


FIG. 16. Hydrodynamic variables for the $n=1$ Dyakonov–Shur mode, $\Delta=2$.

and one is backward, at high enough frequencies there are two forward and two backward waves. This is an important characteristic of the wave dispersion, since it distinguishes a

(a)



(b)

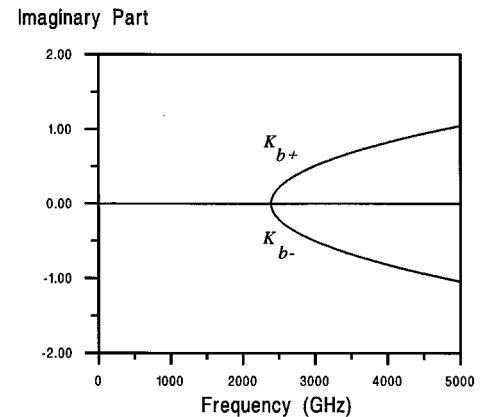
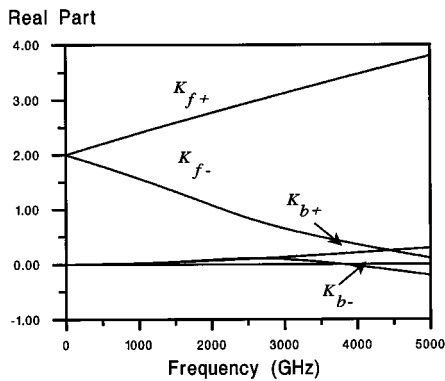


FIG. 17. Bulk dispersion relation roots for deep-water plasmons. The HEMT parameters are the same as in Fig. 6, with a relaxation time $\tau=10^{-7}$ s (corresponding to a collisionless 2DEG). (a) Real part of the roots; (b) imaginary part.

(a)



(b)

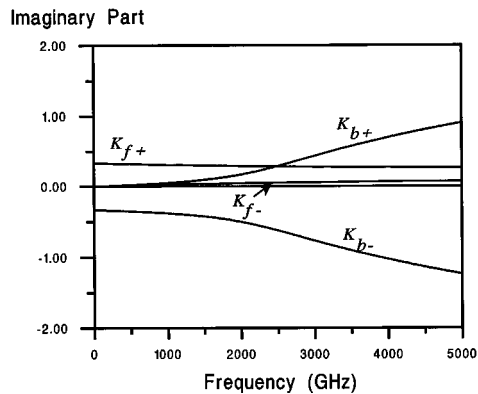


FIG. 18. Bulk dispersion relation roots for deep-water plasmons. The HEMT parameters are the same as in Fig. 6, with a relaxation time $\tau = 10^{-13}$ s (corresponding to a GaAs mobility of $2600 \text{ cm}^2/\text{V s}$.) (a) Real part of roots; (b) imaginary part.

wave that is convectively unstable (spatially growing) from one that is simply a backward decaying wave.¹⁶

Turning to the resonator problem, the same algebraic manipulations as before (see the Appendix) eventually yield the dispersion relation

$$(\theta + z) \left(\frac{\sin \Delta \sqrt{\theta^2 + 2z}}{\sqrt{\theta^2 + 2z}} \cos \Delta \sqrt{\theta^{*2} - 2z} \right) + (\theta^* - z) \times \left(\frac{\sin \Delta \sqrt{\theta^{*2} - 2z}}{\sqrt{\theta^{*2} - 2z}} \cos \Delta \sqrt{\theta^2 + 2z} \right) + \sin 2\Delta = 0,$$

where $\theta = 1 + i\nu_0/\Lambda\tau$. As $\tau \rightarrow \infty$, this expression is easily seen to reduce to the undamped case.

Note that, if we set $z = i\zeta$, where ζ is a real number, we obtain a class of solutions to the completely *real* equation

$$2 \operatorname{Re} \left\{ (\theta + i\zeta) \frac{\sin \Delta \sqrt{\theta^2 + 2i\zeta}}{\sqrt{\theta^2 + 2i\zeta}} \cos \Delta \sqrt{\theta^{*2} - 2i\zeta} \right\} + \sin 2\Delta = 0. \quad (2)$$

If only the ranges where z is pure imaginary are of interest, this real equation can be solved easily with a root finder; the results are shown in Fig. 19 for the four choices $\tau = 10^{-11}$,

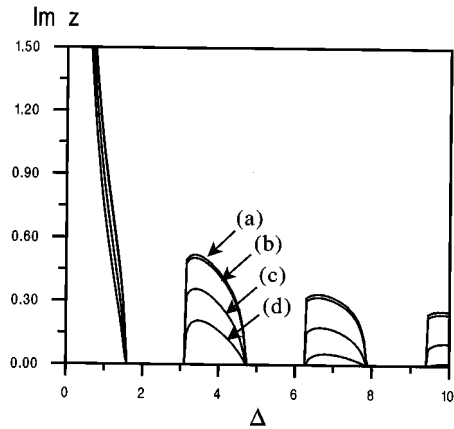


FIG. 19. Effect of dissipation on $\operatorname{Im} z$ for various values of the relaxation time: (a) $-\tau = 10^{-11}$ s, (b) $-\tau = 10^{-12}$ s, (c) $-\tau = 10^{-13}$ s, (d) $-\tau = 5 \times 10^{-13}$ s.

10^{-12} , 10^{-13} , and 5×10^{-14} s, corresponding to mobilities $\mu = 2.6 \times 10^5$, 2.6×10^4 , 2.6×10^3 , and $1.3 \times 10^3 \text{ cm}^2/\text{V s}$. Here the effects of dissipation are obvious: when $\Delta_1 > \pi/2$, the instability gain is rapidly damped away, although it never vanishes completely. This is clearly consistent with the behavior of the bulk dispersion relation.

Another class of solutions to the dispersion relation can be found by setting

$$z = -i\gamma + \zeta,$$

where $\gamma = \nu_0/\Lambda\tau$. Then

$$\theta^2 + 2z = 1 - \gamma^2 + 2\zeta, \quad \theta^{*2} - 2z = 1 - \gamma^2 - 2\zeta.$$

Substituting this expression into Eq. (1) leads to another equation with purely real parameters:

$$(1 + \zeta) \left(\frac{\sin \Delta \sqrt{R^2 + 2\zeta}}{\sqrt{R^2 + 2\zeta}} \cos \Delta \sqrt{R^2 - 2\zeta} \right) + (1 - \zeta) \times \left(\frac{\sin \Delta \sqrt{R^2 - 2\zeta}}{\sqrt{R^2 - 2\zeta}} \cos \Delta \sqrt{R^2 + 2\zeta} \right) + \sin 2\Delta = 0,$$

where $R^2 = 1 - \gamma^2 = |\theta|^2$. For $R = 1$ we recover the original Eq. (1). Again there are special values of Δ for which $\zeta = 0$ is a solution, given by the equation

$$\frac{\sin 2\Delta R}{R} + \sin 2\Delta = 0.$$

These results explain the existence of purely real and purely imaginary solutions to the dispersion relation; however, the full simplex-based calculation shows that they do not account for all of its roots.

VII. CONCLUSIONS

The purpose of this article is to lay some groundwork for a more detailed understanding of the Dyakonov–Shur instability of a 2DEG by removing some of the assumptions inherent in its original formulation. Because of the complexity of the resulting dispersion relations, it appears that considerable numerical work will be required to reveal the true nature

of these plasma disturbances. The issue of what are the “correct” boundary conditions is far from settled; in particular, the vanishing-density “ohmic” conditions need to be looked at. It is possible that some of these issues may be amenable to experimental test in the future.

It is also worth noting that the gateless case treated in detail here is not much different from that of an “ungated” HEMT, for which the 2DEG dispersion relation can be shown to be

$$(\omega \pm K v_0)^2 = \frac{n_0 e^2}{2 \epsilon m} K \left[1 - \left(\frac{\tilde{\epsilon} - \epsilon}{\tilde{\epsilon} + \epsilon} \right) e^{-2Kh} \right].$$

Here $\tilde{\epsilon}$ and ϵ are the dielectric constants of the vacuum above the HEMT and the GaAs, respectively. We can replace the vacuum with a perfect conductor by letting $\tilde{\epsilon} \rightarrow \infty$, which recovers the gated-HEMT expression. However, for the ungated case, in the limit $Kh \ll 1$ this relation becomes

$$(\omega \pm K v_0)^2 = \frac{n_0 e^2}{(\tilde{\epsilon} + \epsilon)m} K,$$

i.e., for small K the Dyakonov–Shur result is not recovered and the 2DEG does indeed look like the deep-water case.

ACKNOWLEDGMENTS

In conclusion, the author would like to acknowledge with gratitude the generosity of Dr. Michael Shur for his valuable comments and willingness to share information about this problem with him. He would like to thank the Physical Sciences Branch of the Army Research Laboratory for their hospitality and the Electronics Division of the Army Research Laboratory for their financial support of this work under the MRCP program (Cooperative Agreement No. DAAL 01-95-2-3530).

APPENDIX

For notational simplicity let us write

$$x = K_{f-}, y = K_{f+}, z = K_{b-}, w = K_{b+}$$

and

$$a = \zeta_{f+}, b = \zeta_{f-}, c = \zeta_{b+}^*, d = \zeta_{b-}^*$$

Then the determinant can be rewritten as follows:

$$\begin{vmatrix} x-y & y+z & y+w \\ a-b & b-c & b-d \\ ax-by & by-cz & by-dw \end{vmatrix} = 0.$$

After some algebra, this becomes

$$\begin{aligned} & bd(y-w)(x+z) + bc(x+w)(z-y) + cd(x-y)(w-z) \\ & + ab(w-z)(y-x) + ad(y+z)(w-x) + ac(y+w)(x-z) = 0. \end{aligned}$$

Liberal use of the identity $K_{f+}K_{f-} = K_{b+}K_{b-} = \omega^2/v_0^2$ lets us write

$$(y-w)(x+z) = yz - xw,$$

$$(x+w)(z-y) = xz - yw,$$

$$(y+z)(w-x) = yw - xz,$$

$$(y+w)(x-z) = wx - yz,$$

and the determinant eventually becomes

$$(bd - ac)(yz - wx) + (ad - bc)(yw - xz) + (cd - ab)$$

$$(x-y)(w-z) = 0.$$

Let us write

$$K_{f+} = A_f + B_f,$$

$$K_{f-} = A_f - B_f,$$

$$K_{b+} = A_b + B_b,$$

$$K_{b-} = A_b - B_b,$$

where $A_f = \xi + k_0$, $A_f = \xi - k_0$, $B_f = \sqrt{\xi(\xi + 2k_0)}$, and $B_f = \sqrt{\xi(\xi - 2k_0)}$. Then combining the ζ_i into trigonometric functions gives

$$\begin{aligned} & (wx - yz) \sin[(B_f - B_b)L] + (wy - xz) \sin[(B_f + B_b)L] \\ & - (x - y)(w - z) \sin[(A_f + A_b)L] = 0. \end{aligned}$$

Using the usual trigonometric identities transforms this equation to the form

$$\begin{aligned} & (w - z)(y + x) \sin B_f L \cos B_b L + (w + z)(y - x) \cos B_f L \\ & \times \sin B_b L - (x - y)(w - z) \sin[(A_f + A_b)L] = 0. \end{aligned}$$

But,

$$y + x = 2A_f,$$

$$y - x = 2B_f,$$

$$w + z = 2A_b,$$

$$w - z = 2B_b,$$

which reduces the dispersion relation to

$$\begin{aligned} & A_f B_b \sin(B_f L) \cos(B_b L) + B_f A_b \cos(B_f L) \sin(B_b L) \\ & + B_f B_b \sin[(A_f + A_b)L] = 0, \end{aligned}$$

or

$$\begin{aligned} & A_f \frac{\sin(B_f L)}{B_f} \cos(B_b L) + A_b \frac{\sin(B_b L)}{B_b} \cos(B_f L) \\ & + \sin[(A_f + A_b)L] = 0. \end{aligned}$$

Setting $A_f + A_b = 2\xi$ recovers the expression given in the main part of the text.

¹M. I. Dyakonov and M. I. Shur, Phys. Rev. Lett. **71**, 2465 (1993).

²L. D. Landau and I. M. Lifshits, *Fluid Mechanics* (Pergamon, New York, 1966).

³A. V. Chaplik, Sov. Phys. JETP **35**, 395 (1972).

⁴M. Nakayama, J. Phys. Soc. Jpn. **36**, 393 (1974).

⁵S. J. Allen, Jr., D. C. Tsui, and R. A. Logan, Phys. Rev. Lett. **38**, 980 (1977).

⁶F. J. Crowne, Phys. Rev. B **24**, 5455 (1980); **27**, 3201 (1982).

- ⁷D. C. Tsui, E. Gornik, and R. A. Logan, Solid State Commun. **35**, 875 (1980).
- ⁸P. Roblin, J. Kang, A. Ketterson, and H. Morkoç, IEEE Trans. Electron Devices **ED-34**, 1919 (1987).
- ⁹T. Ferrel, Phys. Rev. **111**, 2416 (1958).
- ¹⁰A. Fetter, Ann. Phys. (N.Y.) **81**, 367 (1973).
- ¹¹E. I. Adirovich, Sov. Phys. Solid State **2**, 1282 (1960).
- ¹²C. R. Crowell and S. M. Sze, Solid-State Electron. **9**, 1035 (1966).
- ¹³C. R. Crowell and M. Beguwala, Solid-State Electron. **14**, 1149 (1971).
- ¹⁴M. A. Lampert and P. Mark, *Current Injection in Solids* (McGraw-Hill, New York, 1962), Chap. 8.
- ¹⁵T. H. Stix, *The Theory of Plasma Waves* (Academic, New York, 1970).
- ¹⁶F. J. Crowne, J. Appl. Phys. **57**, 4772 (1985).